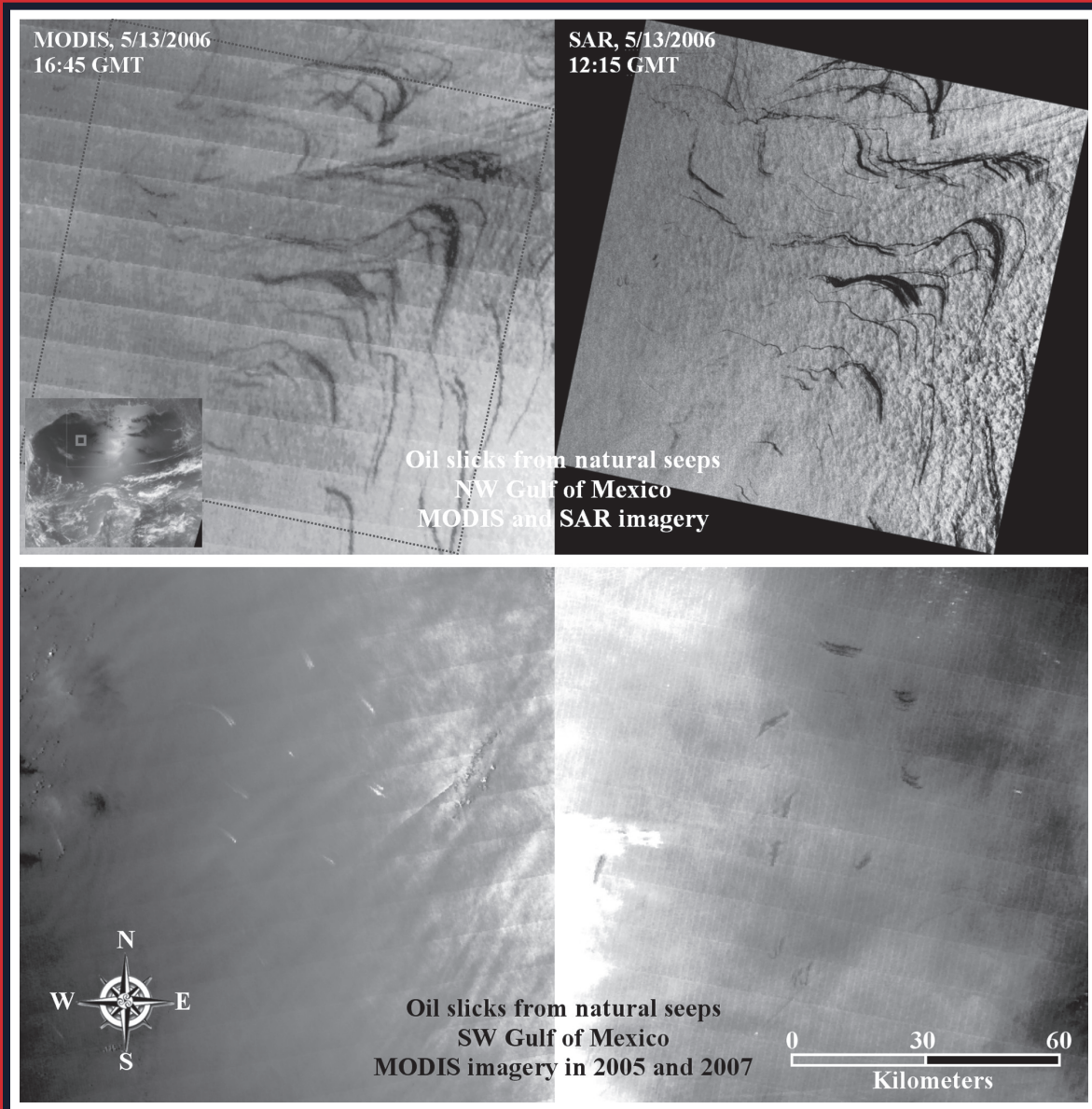


Geophysical Research Letters

16 JANUARY 2009
Volume 36 Number 1
American Geophysical Union



- Natural oil seepage in Gulf of Mexico occurs more often than thought
- Freak waves in moderate Japanese waters may have caused fishing boat sinking
- Fate of climate feedbacks as temperatures warm
- Atmosphere driven by cascades, an aid to numerical weather prediction



Detection of natural oil slicks in the NW Gulf of Mexico using MODIS imagery

Chuanmin Hu,¹ Xiaofeng Li,² William G. Pichel,³ and Frank E. Muller-Karger⁴

Received 24 September 2008; revised 7 November 2008; accepted 24 November 2008; published 6 January 2009.

[1] We demonstrate the unique capability of the MODIS instruments in detecting oil slicks in an open ocean environment. On 13 May 2006, in the NW Gulf of Mexico where water depth ranges from 50 to 2500 m, one 250-m resolution MODIS image showed at least 164 surface slicks under sun glint (glint reflectance, L_g , ranged between 0.0001 and 0.06 sr^{-1}). After discounting other possible causes, we believe these are the result of natural seeps. Our analysis showed total coverage of $\sim 1900 \text{ km}^2$, with individual slicks varying in surface area ($11.7 \pm 14.8 \text{ km}^2$) and length ($19.2 \pm 12.4 \text{ km}$). Concurrent SAR imagery showed similar area estimates to within 30%. This estimate, based on a single image, is higher than earlier estimates from a database of multi-date SAR images for the same region. Inspection of >200 images for the month of May between 2000 and 2008 revealed similar slicks on at least 50 images. On 2 June 2005, slicks were detected under sun glint with both negative contrast ($L_g < 0.05 \text{ sr}^{-1}$) and positive contrast ($L_g > 0.05 \text{ sr}^{-1}$). These slicks could not be detected in glint-free MODIS images collected on the same day. Because of the near-daily revisit and wide sun glint coverage (e.g., $>800 \text{ km}$ E-W between March and October at 25°N), systematic and global application of the MODIS 250-m imagery can help locate natural seeps and improve estimates of seepage rates in the world's ocean.

Citation: Hu, C., X. Li, W. G. Pichel, and F. E. Muller-Karger (2009), Detection of natural oil slicks in the NW Gulf of Mexico using MODIS imagery, *Geophys. Res. Lett.*, 36, L01604, doi:10.1029/2008GL036119.

1. Introduction

[2] Crude oil from natural seeps on the ocean's floor represents an important source of oil to the sea [*National Research Council*, 2003]. Natural seepage accounts for $\sim 47\%$ of the crude oil entering the marine environment, but these numbers have large uncertainties [*Kvenvolden and Cooper*, 2003]. Timely and accurate detection of surface slicks can improve estimates of seepage rate and help monitor oil spills and manage coastal resources.

[3] Assessment of the distribution and fate of oil slicks on the ocean's surface is often accomplished with use of remote sensing techniques. Satellite remote sensing may

be "the best approach to more accurate estimates" of natural oil seepage rates [*Kvenvolden and Cooper*, 2003]. These techniques typically include visible, infrared, microwave, and radar sensors (see reviews by *Fingas and Brown* [2000] and *Brekke and Solberg* [2005]). However, most of these estimates, as well as detection of spills from other sources, have relied on Synthetic Aperture Radar (SAR) data [e.g., *MacDonald et al.*, 1996; *Liu et al.*, 2000], which are limited by coverage, revisit frequency, and cost. High-resolution visible images from airborne photographs or from Landsat TM/ETM+ sensors have been used as proof of concept [*MacDonald et al.*, 1993], but these also have similar limitations.

[4] *Hu et al.* [2003] first used operational satellite data from MODIS (Moderate Resolution Imaging Spectroradiometer) [*Esaias et al.*, 1998] to detect and monitor oil spills in a turbid estuary, where MODIS demonstrated the advantages of several images per week at no cost. However, similar applications in the open ocean environment could not be found in the peer-reviewed literature. Here we show that MODIS is capable of detecting oil slicks even in the clearest ocean water, based not on the optical properties of oil slicks but on the same backscattering principles of SAR. We use MODIS imagery to estimate the surface area of natural oil slicks in the NW Gulf of Mexico (GOM), and argue that oil seepage rates in this region need to be revisited.

2. Methods

[5] MODIS Level-0 data were obtained from NASA/GSFC and processed to Level-1b (calibrated total radiance) using the SeaWiFS Data Analysis System (SeaDAS version 5.1). They were then corrected for Rayleigh scattering and registered to a cylindrical equidistant projection. Digital data were stored in HDF files, and 250-m resolution Red-Green-Blue images were generated using data from the 645-, 555-, and 469-nm bands, respectively. The 500-m resolution data at 555- and 469-nm were interpolated to 250-m resolution using a sharpening scheme similar to that used for Landsat. Because of the compromise between dynamic range and sensitivity in composing the RGB images, the software ENVI (Environment for Visualizing Images, version 4.2) was used to enhance image contrast to facilitate visualization and analysis. The same analysis can also be performed with other software packages (e.g., ArcInfo).

[6] Sun glint reflectance, L_g (sr^{-1}), was estimated using the *Cox and Munk* [1954] model and wind data from the National Centers for Environmental Prediction (NCEP) and solar/viewing geometry from MODIS [*Wang and Bailey*, 2001].

¹College of Marine Science, University of South Florida, St. Petersburg, Florida, USA.

²IMSG at NOAA/NESDIS, Camp Springs, Maryland, USA.

³NESDIS, NOAA, Camp Springs, Maryland, USA.

⁴School for Marine Science and Technology, University of Massachusetts Dartmouth, New Bedford, Massachusetts, USA.

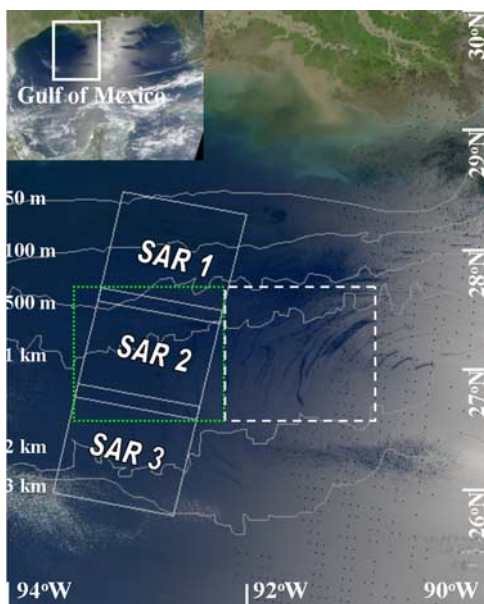


Figure 1. MODIS/Terra RGB image of 13 May 2006 (16:45 GMT) covering the Gulf of Mexico (inset), with bathymetry isobaths from 50 to 3000 m annotated. The locations of 3 SAR images collected on the same day (12:15 GMT) are outlined; “SAR 2” and the corresponding MODIS data (outlined by the dotted box) were analyzed in detail (Figure 2). Note that the surface slicks under ambient sun glint (to the east of the image) are clearly visible even without color stretch. The glint patterns in the eastern GOM are due to changes in wind speed (which changes surface roughness) and ocean currents.

[7] SAR data from RADARSAT-1 (a C-band radar with horizontal polarization and 100-km swath width) were obtained during the Alaska SAR Demonstration (AKDEMO) project. These 25-m resolution images were standard beam mode scenes, processed at the Alaska Satellite Facility (ASF) at the University of Alaska, Fairbanks. The images were navigated and analyzed using ENVI.

3. Results

[8] A MODIS/Terra image on 13 May 2006 contained significant sun glint in the GOM, where three SAR images were collected 4.5 hours earlier (Figure 1). Within 2° longitude to the east of the SAR scenes, surface slicks were apparent in the MODIS sun glint area even without contrast enhancement.

[9] All three SAR images showed surface slicks due to reduced radar backscattering. Most of these slicks were also clearly visible in the MODIS image (see Figure 2 for an example. Note that due to limitations of the printing matter, the full-resolution MODIS imagery are available online in the auxiliary material).¹ The slight difference in slick shape and position was effected by winds and ocean currents in the time elapsed between the two satellite overpasses. Similar patterns were observed in the other two SAR-MODIS image pairs outlined in Figure 1.

¹Auxiliary materials are available in the HTML. doi:10.1029/2008GL036119.

[10] To determine which MODIS band showed the best contrast between the surface slick and surrounding clear-ocean water, we extracted MODIS and SAR data along several virtual transect lines, one of which is along 92.76°W (Figure 2). Figure 3 shows three slicks of decreased backscattering signal among the highly speckled (noisy) SAR data. The two 250-m MODIS bands showed excellent contrast (about -0.2 , defined as $(R_s - R_c)/R_c$ where “s” and “c” stand for slick and clear water, respectively), sufficient to detect the slicks seen in the SAR data. Indeed, slick #2 in Figure 3 was only about 75 to 100 m wide in the SAR image, yet it was successfully captured in the MODIS 250-m data. The 500-m resolution blue and green bands (469- and 555-nm) as well as the short-wave bands between 1240- and 2130-nm showed lower spectral and spatial contrast, and were not as useful to detect the slicks, often <1 km in width.

[11] The total surface area covered by the slicks was estimated semi-objectively by combining visual inspection, manual delineation, and threshold separation. For the study region shown in Figure 1, Table 1 shows the statistics of the slicks identified in the MODIS image.

[12] A natural question is whether the estimates shown in Table 1, based on the MODIS data, are accurate. We tested the results against the concurrent SAR images. The “SAR 2” image (Figure 2 (right)) showed surface slicks covering about 707 km^2 , while the MODIS data (Figure 2 (left)) showed slicks covering 923 km^2 . We believe this difference may be due to the coarser resolution of the MODIS data (250 m compared to 25 m for SAR), and that some of the MODIS pixels were actually mixed substrate with oil and non-oil waters. This resulted in a $\sim 30\%$ overestimate. Hence, the total slick area for the study region shown in Figure 1 (Table 1) is likely to be smaller and closer to about 1500 km^2 .

[13] The remarkable similarity between the observed patterns in MODIS and SAR images results from the same physical principles: the modulation (damping) of the sea surface roughness and backscattering/reflectance of electromagnetic radiation by the slicks. While this modulation can almost always be observed by SAR under optimal wind conditions between 3 and 10 m s^{-1} [Simecek-Beatty and Pichel, 2006], in visible imagery it can only be observed under conditions of sun glint. In the MODIS image collected on 13 May 2006 (Figure 1), slicks were identified when the glint reflectance, L_g , varied between 0.0001 sr^{-1} to the west and 0.06 sr^{-1} to the east. This is different from the oil spill event in a turbid estuary [Hu et al., 2003] where oil spills affected the optical properties of the water column [Otremba and Piskozub, 2004, and references therein] and therefore the oil slicks could be observed without sun glint in MODIS imagery. It is likely that the slicks we observed here are very thin, and therefore had no clear effect on the optics of the water column. Indeed, the MODIS image collected with the Aqua satellite in the afternoon had no glint, and showed no contrast changes in the area of the slicks.

4. Discussion

[14] What could cause the observed slicks? Freshwater runoff and surfactants from phytoplankton blooms can

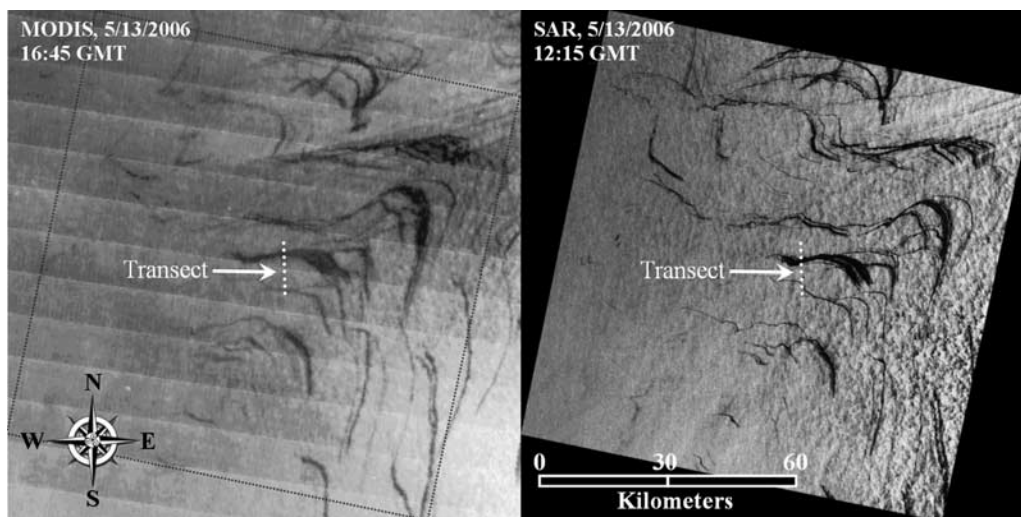


Figure 2. (left) MODIS RGB image (after contrast enhancement) and (right) SAR image for the area outlined as “SAR 2” in Figure 1. The area is between 26.58°N – 27.68°N and 93.43°W – 92.21°W . Data along the virtual transect line were extracted and analyzed (Figure 3). Our analysis resulted in slick areas of $\sim 923 \text{ km}^2$ as estimated using the MODIS image (bounded by the dotted outline) and $\sim 707 \text{ km}^2$ from the SAR image (see text for details). These surface slicks did not show on another cloud-free and glint-free MODIS image from the Aqua satellite collected 3 hours later.

dampen sea surface roughness [e.g., *Lin et al.*, 2002; *DiGiacomo et al.*, 2004]. These phenomena are sometimes difficult to distinguish from oil spills [*Alpers and Espedal*, 2004]. The slicks we observed in this study were located far away from land runoff and over water depths of 50–2000 m. The glint-free MODIS/Aqua data on the same day showed clear waters in this region (chlorophyll-*a* concentration $\sim <0.1 \text{ mg m}^{-3}$), discounting the possibility of phytoplankton blooms. The Constant False Alarm Rate ship detection algorithm [*Wackerman et al.*, 2001] showed only a few ships from the concurrent SAR data, suggesting that the slicks were not caused by oil spills from such vessels or oils released as a result of fishing activity. Indeed, the study area is known to have natural oil seeps [*MacDonald et al.*, 1996]. Examination of other MODIS imagery showed that the slicks were recurrent in the same locations. Therefore, we believe that most, if not all, observed slicks were from natural seeps in this region.

[15] The capability of SAR for detection of oil slicks is well known [*Liu et al.*, 2000] and has received wide applications in spill mapping and monitoring. In contrast, only a handful of studies using visible imagery have been reported in the literature, possibly due to the sporadic nature of high-resolution airborne photography and satellite imagery (e.g., Landsat, IKONOS, AVIRIS) and due to the difficulty in identifying slicks in visible imagery. With all these means combined, it has been difficult to provide a complete, snapshot picture for the 300-km by 300-km area where oil slicks were identified (Table 1). This is because the slicks have relatively short half lives (e.g., 6–48 hours [*MacDonald et al.*, 1993]) due to evaporation and degradation, while the coverage of the above sensors is limited and revisit frequency is very low (e.g., 16 days for Landsat, 100-km swath for SAR “standard mode”). In contrast, in subtropical and tropical regions between spring and fall, a significant portion of the MODIS 2330-km swath is “contaminated” by sun glint. For example, assuming 5 m s^{-1}

wind, at 25°N (center of the GOM) $>800 \text{ km}$ of the MODIS swath was found to have $L_g > 0.0001 \text{ sr}^{-1}$ between March and October (Figure 4 (inset)), making oil slick detection possible. The combination of the two MODIS instruments in the morning (Terra) and afternoon (Aqua) assures repeated glint coverage every 2–3 days. This wide glint coverage, combined with the $36.5 \pm 15.1\%$ cloud-free chance for the entire GOM on a daily basis (Figure 4 (inset)), can greatly

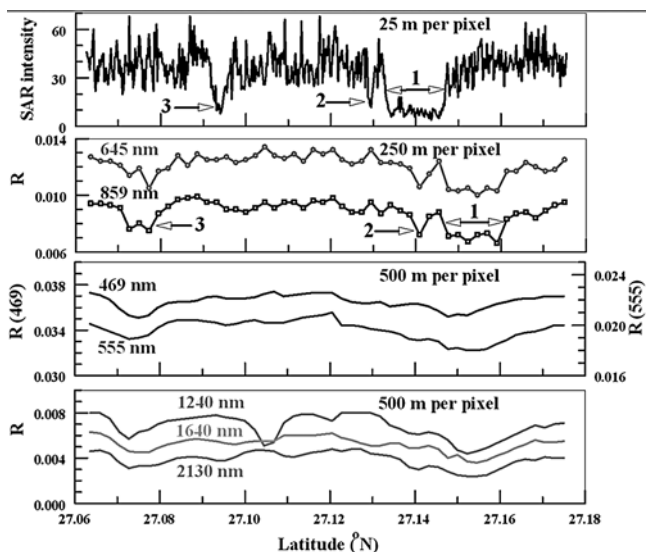


Figure 3. SAR and MODIS data along the virtual transect line in Figure 2. SAR data are presented as relative numbers, while MODIS data are the Rayleigh-corrected reflectance (R). Three surface slicks, identified from both MODIS and SAR images (Figure 2), are annotated here with the numerals 1, 2, and 3. Note that due to the 4.5-hour difference, the positions of the slicks shifted under influence of wind and currents between the two images.

Table 1. Statistics of Individual Surface Slicks Identified in the MODIS Image Shown in Figure 1^a

	Mean	SD	Min	Max
Length (km)	19.2	12.4	2.3	52.8
Width (km)	0.65	0.63	0.12	4.6
Area (km ²)	11.7	14.8	0.06	106.7

^aFor the area 25.69°N–28.62°N; 90.14°W–93.58°W. The total number of slicks counted was 164, with a grand total area of 1,920 km². The estimate from the concurrent SAR images was ~1500 km².

enhance our capability to detect large slicks at low latitudes. For instance, the MODIS image in Figure 1 showed at least 1500 km² surface area covered by the oil slicks (after adjustment from SAR validation). This figure is higher than previous estimates (~1000 km²) during an aggregate survey of the northern GOM using multiple satellite images [Mitchell *et al.*, 1999], possibly due to the non-simultaneous measurements from multi-date images in the earlier study.

[16] The natural oil slicks should be observable in other MODIS images under optimal conditions (sun glint but cloud free). Although a systematic analysis is still underway, opportunistic examination of >200 MODIS images for the month of May between 2000 and 2008 revealed similar slicks in at least 50 images, confirmed by several concurrent SAR images. Most slicks are recurrent in the same locations in the western GOM, indicating natural seeps. Due to the limited information from the published literature, however, it is unclear if any of the identified seeps in the NW and SW GOM are “new”.

[17] Some images showed both negative (as in Figures 1 and 2) and positive slick contrasts. While the full-resolution MODIS images are available online in the auxiliary material to show these features in detail, Figure 4 shows an example of these opposite contrasts. The hook-shaped slicks occurred in the entire 240 km × 120 km region and covered a much larger area outside this region (not shown here). The oil slick contrast changed from negative (dark) in the west to positive (bright) in the east. Similar negative-positive changes were observed in space shuttle photographs [MacDonald *et al.*, 1993] and many of the MODIS images we examined in this region, and reported in satellite imagery from MODIS [Hu *et al.*, 2003] and the Multi-angle Imaging SpectroRadiometer in a turbid estuary [Chust and Sagarminaga, 2007]. The slicks with positive contrast might be falsely interpreted as floating *Sargassum* in this region [Gower *et al.*, 2006], but this possibility could be easily ruled out with repeated imagery showing slicks with negative contrast in the same locations.

[18] The negative contrast can be explained as a reduction in glint due to dampening of the surface roughness, while the positive contrast results from higher specular reflection within the oil film patch. By comparing the contrast patterns and θ_m (the angle between the viewing direction and the direction of mirror reflection; see Figure 4 (inset)) for the entire GOM, we estimated that the contrast changed sign at $\theta_m \approx 12^\circ$, where L_g was about 0.05 sr^{-1} . For the image shown in Figure 1, several slicks with positive contrast also occurred in the south with $\theta_m < 12^\circ$ and $L_g > 0.05 \text{ sr}^{-1}$. Analysis of other MODIS images suggested that the contrast changes sign for θ_m between

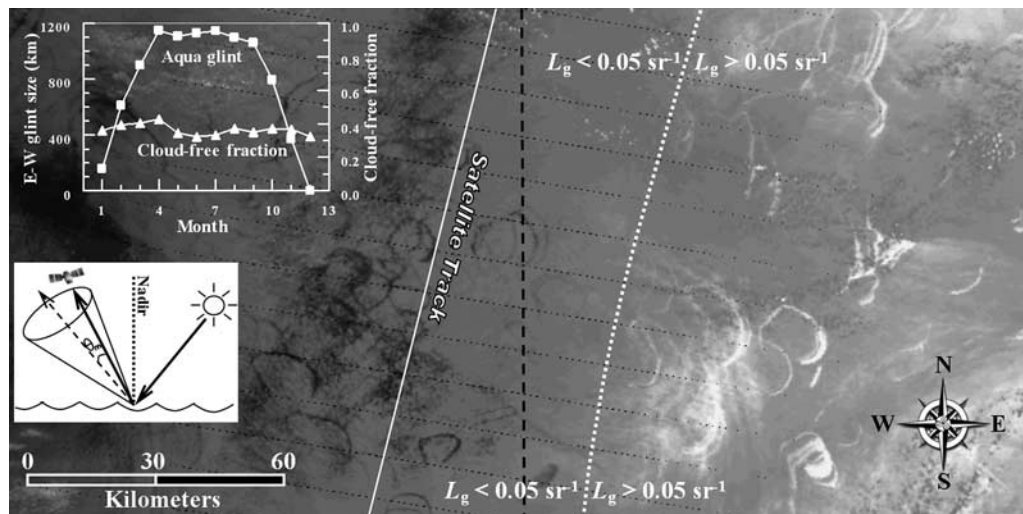


Figure 4. MODIS/Terra RGB image on 2 June 2005 (16:55 GMT) for the area delineated by the dotted and dashed boxes in Figure 2 (26.58°N–27.68°N and 93.43°W–90.98°W.), separated by the dashed line. The satellite track shows the nadir view, while the dotted line denotes the glint reflectance of 0.05 sr^{-1} where the slick contrast changes from negative (darker) to positive (brighter). This is corresponding to $\theta_m \approx 12^\circ$, where θ_m is the angle between the viewing direction and the direction of mirror reflection (dashed arrow in the inset). $\cos(\theta_m) = \cos(\theta_0)\cos(\theta) - \sin(\theta_0)\sin(\theta)\cos(\phi)$, where θ_0 , θ , and ϕ are the solar zenith, satellite zenith, and relative azimuth angles, respectively. The large dark patches in the west are not due to oil films but a result of low atmosphere/ocean radiance and color stretching. Note that the figure is only a small subset of the MODIS image, with the latter available online in the auxiliary material showing much more extensive oil slicks. (inset) Seasonal glint coverage (glint defined as $L_g > 0.0001 \text{ sr}^{-1}$) in the MODIS/Aqua swath at 25°N assuming wind speed = 5 m s^{-1} . Results for MODIS/Terra are nearly identical. Also shown in the inset figure is the cloud-free possibility for the entire GOM estimated from 11-year SeaWiFS data (1997–2008).

12° and 14° and L_g between 0.04 and 0.05 sr^{-1} . However, whether this observation can be generalized still needs further research, including a simulation study with bi-directional optical properties of the oil film [e.g., *Otremba and Piskozub*, 2004].

5. Conclusion

[19] The unique capability of the MODIS instruments in detecting oil slicks in an oligotrophic ocean has been demonstrated. The image pairs from concurrent MODIS and SAR measurements prove the ability to examine large areas for oil slicks using MODIS. MODIS helps by expanding the coverage and revisit frequency. Our results suggest that annual seepage rates in the northwestern Gulf of Mexico may have been underestimated in past studies, but a systematic examination of an extensive MODIS time series is required to assess annual slick formation rates. Because of the global availability of the medium-resolution (250-m and 500-m) MODIS data and their consistent coverage of sun glint in tropical and subtropical regions, systematic application may also improve the estimation of global annual seepage rates and help identify new oil seeps.

[20] **Acknowledgments.** This work was supported by the U.S. NOAA (NA06NES4400004) and NASA (NNS04AB59G). We thank the NASA/GSFC for providing MODIS data and software. SAR data were obtained under the NASA RADARSAT-0011-0071 and NOAA/NESDIS/STAR Ocean Remote Sensing programs. The views, opinions, and findings contained in this report are those of the authors and should not be construed as an official NOAA or U.S. Government position, policy, or decision. IMaRS contribution 128.

References

- Alpers, W., and H. A. Espedal (2004), Oils and surfactants, in *Synthetic Aperture Radar Marine User's Manual*, edited by C. R. Jackson and J. R. Apel, pp. 263–275, U.S. Dep. of Commer., Washington, D. C.
- Brekke, C., and A. H. S. Solberg (2005), Oil spill detection by satellite remote sensing, *Remote Sens. Environ.*, *95*, 1–13.
- Chust, G., and Y. Sagarminaga (2007), The multi-angle view of MISR detects oil slicks under sun glitter conditions, *Remote Sens. Environ.*, *107*, 232–239.
- Cox, C., and W. H. Munk (1954), The measurement of the roughness of the sea surface from photographs of the sun's glitter, *J. Opt. Soc. Am.*, *44*, 838–850.
- DiGiacomo, P. M., L. Washburn, B. Holt, and B. H. Jones (2004), Coastal pollution hazards in southern California observed by SAR imagery: Stormwater plumes, wastewater plumes, and natural hydrocarbon seeps, *Mar. Pollut. Bull.*, *49*, 1013–1024.
- Esaias, W. E., et al. (1998), An overview of MODIS capabilities for ocean science observations, *IEEE Trans. Geosci. Remote Sens.*, *36*, 1250–1265.
- Fingas, M., and C. Brown (2000), Oil-spill remote sensing—An update, *Sea Technol.*, *41*, 21–26.
- Gower, J., C. Hu, G. Borstad, and S. King (2006), Ocean color satellites show extensive lines of floating *Sargassum* in the Gulf of Mexico, *IEEE Trans. Geosci. Remote Sens.*, *44*(12), 3619–3625, doi:10.1109/TGRS.2006.882258.
- Hu, C., F. E. Müller-Karger, C. Taylor, D. Myhre, B. Murch, A. L. Odriozola, and G. Godoy (2003), MODIS detects oil spills in Lake Maracaibo, Venezuela, *Eos Trans. AGU*, *84*(33), doi:10.1029/2003EO330002.
- Kvenvolden, K. A., and C. K. Cooper (2003), Natural seepage of crude oil into the marine environment, *Geo Mar. Lett.*, *23*, 140–146.
- Lin, I.-I., L. Wen, K. Liu, W. Tsai, and A. K. Liu (2002), Evidence and quantification of the correlation between radar backscatter and ocean colour supported by simultaneously acquired in situ sea truth, *Geophys. Res. Lett.*, *29*(10), 1464, doi:10.1029/2001GL014039.
- Liu, A. K., S. Y. Wu, W. Y. Tseng, and W. G. Pichel (2000), Wavelet analysis of SAR images for coastal monitoring, *Can. J. Remote Sens.*, *26*, 494–500.
- Macdonald, I. R., N. L. Guinasso Jr., S. G. Ackleson, J. F. Amos, R. Duckworth, R. Sassen, and J. M. Brooks (1993), Natural oil slicks in the Gulf of Mexico visible from space, *J. Geophys. Res.*, *98*, 16,351–16,364.
- MacDonald, I. R., et al. (1996), Remote sensing inventory of active oil seeps and chemosynthetic communities in the northern Gulf of Mexico, in *Hydrocarbon Migration and Its Near-Surface Expression*, edited by D. Schumacher and M. A. Abrams, *AAPG Mem.*, *66*, 27–37.
- Mitchell, R., I. R. MacDonald, and K. Kvenvolden (1999), Estimates of total hydrocarbon seepage into the Gulf of Mexico based on satellite remote sensing images, *Eos Trans. AGU*, *80*(49), Ocean Sci. Meet. Suppl., Abstract OS411-02.
- National Research Council (2003), *Oil in the Sea III: Inputs, Fates, and Effects*, Natl. Acad. Press, Washington, D. C.
- Otremba, Z., and J. Piskozub (2004), Modelling the bidirectional reflectance distribution function (BRDF) of seawater polluted by an oil film, *Opt. Express*, *12*, 1671–1676.
- Simecek-Beatty, D., and W. Pichel (2006), RADARSAT-1 synthetic aperture radar analysis for M/V Selendang Ayu oil spill, paper presented at the 29th Arctic and Marine Oil spill Program Technical Seminar, Environ. Can., Vancouver, B. C., Canada, 6–8 June.
- Wackerman, C. C., K. S. Friedman, W. G. Pichel, P. Clemente-Colon, and X. Li (2001), Automatic Detection of Ships in RADARSAT-1 SAR imagery, *Can. J. Remote Sens.*, *27*, 568–577.
- Wang, M., and S. W. Bailey (2001), Correction of sun glint contamination on the SeaWiFS ocean and atmosphere products, *Appl. Opt.*, *40*, 4790–4798.

C. Hu, College of Marine Science, University of South Florida, 140 Seventh Avenue, South, St. Petersburg, FL 33701, USA. (hu@marine.usf.edu)

X. Li and W. G. Pichel, NESDIS, NOAA, 5200 Auth Road, Camp Springs, MD 20746, USA.

F. E. Muller-Karger, School for Marine Science and Technology, University of Massachusetts Dartmouth, 706 South Rodney French Boulevard, New Bedford, MA 02744, USA.